Colorimetric Prediction of Halftone Prints with Pale-ink Model

Masaru Kato[*1], Masao Inui[*2], and Yoshihiko Azuma[*3]

Abstract In the offset processes or digital printing, photographic images are printed onto paper by converting them into halftone dot patterns. Dot size is measured in terms of dot area. The difference in dot area between an original dot and its reproduction is called dot gain. In this study, we create a model in which pale-ink is introduced in consideration of light scattering term and investigate the validity of the model. The pale-ink reflectance spectrum is estimated based on the modified Beer-Lambert law, which was introduced to estimate the attenuation of light for scattering media. The path length factor and scattering loss factor are estimated from the modified Beer-Lambert law. In the pale-ink model, the spectral reflectance of the pale-ink, solid area, and paper substrate are converted to *XYZ* tristimulus values, and the actual colour is predicted by a linear combination of weighted tristimulus values. We attempted to predict dot gain using our pale-ink model and found that our proposed model offered improved prediction accuracy over the conventional Murray-Davies and Yule-Nielsen models.

1. Introduction

In the offset processes or digital printing, photographic images are printed onto paper by converting them into halftone dot patterns. Dot size is measured in terms of dot area. The difference in dot area between an original dot and its reproduction is called dot gain, and it should be noted that variations of approximately 3% in either growth or reduction of a dot area will be sufficient to cause a noticeable change in the tone or hue of a reproduced image.

The Murray-Davies model (Eq. 1) describes image reflectance as a linear combination of ink dot and paper reflectance [1]. However, the reflectance values calculated using the Murray-Davies formula do not always coincide with the measured values.

$$R = a_S R_S + (1 - a_S) R_p \tag{1}$$

where R is predicted spectral reflectance, a_s is fractional dot area of the ink, R_s is the spectral reflectance of the ink at solid (full coverage), and R_p is the spectral reflectance of the paper substrate.

Yule and Nielsen, in their model (Eq. 2), interpreted the discrepancies as the result of light penetration and scattering in the paper substrate [2].

$$R = \left[a_S R_S^{1/n} + (1 - a_S) R_p^{1/n} \right]^n \tag{2}$$

where n is a parameter accounting for light spreading in paper, and all other variables are as described above.

Their theoretical analysis showed that the nonlinear relationship between measured and predicted reflectance could be described well using a power function. The n value of the Yule-Nielsen model, which is compatible with offset printing, is known to be n = 1.7 [3]. This provides a numerical approximation, but does not provide any physical insight into the actual constituent materials.

Equation (3) can be obtained by inserting 2 into n of equation (2). Thus, the Yule-Nielsen model contains, in the second term, the square root of the product of the reflectance of ink and the reflectance of the paper substrate. The second term of equation (3) corresponds to the optical dot gain, which is the

[*1] Part-time lecturer, Department of Media and Image Technology, Faculty of Engineering, Tokyo Polytechnic University,
[*2] Professor, Department of Media and Image Technology, Faculty of Engineering, Tokyo Polytechnic University,
[*3] Lecturer, Department of Media and Image Technology, Faculty of Engineering, Tokyo Polytechnic University,
Received Sept. 21, 2011

scattering component of a halftone dot.

$$R = a_S^2 R_S + 2a_S(1-a_S)\sqrt{R_S R_p} + (1-a_S)^2 R_p \quad (3)$$

We studied the causes of dot gain deviations using a halftone dot representation based on the Murray-Davies model. Our core-fringe model assumes that a halftone dot consists of two regions; a central core area that contains a solid ink layer of equal thickness, and a marginal fringe area that has a thinner ink layer [4]. This model can describe the non-linear behaviour of single-ink halftone prints as well as predict the spectral reflectance more precisely than the Murray-Davies model. Furthermore, we think that evaluating dots from their colorimetric characteristics can be helpful when attempting to intuitively understand the effect of dot gain on hue. In this study, we create a model in which pale-ink is introduced in consideration of the second term of equation (3) and the core-fringe model, and investigate the validity of the model. Our goal is the development of a generally usable model by examining the ways in which the material characteristics are considered.

2. Model creation by the introduction of pale-ink

The variables and constants used in this model were selected to develop physically based approaches. In the pale-ink model, the spectral reflectance of the pale-ink, solid area, and paper substrate are converted to *XYZ* tristimulus values, and the actual colour is predicted by a linear combination of weighted tristimulus values. To develop the pale-ink model, we used offset prints spectral reflection data in the Standard object colour spectra (SOCS) database [5].

2.1 Modified Beer-Lambert Model

The effect of optical dot gain depends on the length of the lateral scattering of light within the substrate and the size of the halftone dots. For scattering media, the modified Beer-Lambert law was introduced to estimate the attenuation of light, and is commonly used in the field of near-infrared tissue spectroscopy [6].

$$A = \log(I_0 / I) = B\mu_a d + G \quad (4)$$

where term A is the light attenuation between the incident light I_0 and the transmitted light I, μ_a is absorption coefficient, G is the attenuation factor resulting from scattering loss, and B is the path length factor, which, when multiplied by the geometric distance d between the source and detector, accounts for the increase in optical path length caused by scattering.

2.2 Estimation of reflection spectrum of pale-ink

The pale-ink reflectance spectrum is estimated based on the modified Beer-Lambert law. In equation (4), for the solid area we presume absorption coefficient μ_a is constant and d is equivalent to the mean optical path length. Therefore, $\mu_a d$ is assumed to correspond to the attenuation of the solid area. The transmitted light I is considered to be the detected reflected light.

$$I = I_0 R_{pale} \quad (5)$$

By determining B and G in equation (4), the predicted pale-ink reflectance (R_{pale}) can be obtained. In the halftone, the lights transmitted into the layer presumably pass through the ink layer and the paper

substrate due to scattering. The contribution of this light to absorption is expected to be small compared with the solid area. Thus, B is 1 or less ($B \leq 1$). The term B and G in equation (4) are selected so that the squared error sum between the measured reflectance (R_{meas}) at the dot area coverage of 50%, where the dot gain becomes the maximum, and the pale-ink reflectance (R_{pale}) becomes the minimum. In the calculation process of B and G, the calculation range of B can be limited by allowing $G = 0$ and confirming the variation of the squared error sum between R_{meas} and R_{pale}. Then, B and G are determined so that the minimum sum of squared error is attained.

2.3 Pale-ink Model

A model in which pale-ink is integrated into the Murray-Davies equation can be obtained, as shown below, by the conversion of reflectance to tristimulus values.

(a) CIE tristimulus values XYZ $\vec{T}$ of the solid area, paper substrate, and pale-ink are determined from the respective spectral reflectance, R_{solid}, R_{paper}, and R_{pale}.

$$\vec{T} = \begin{bmatrix} X \\ Y \\ Z \end{bmatrix} = k \int P(\lambda) R(\lambda) \begin{bmatrix} \bar{x} \\ \bar{y} \\ \bar{z} \end{bmatrix} d\lambda \qquad (6)$$

Here, $k = 100 / \int P(\lambda)\bar{y}d\lambda$, $P(\lambda)$ represents the relative spectral distribution of the illuminant D_{50}: recommended illuminant for hardcopy viewing (7),(8), $R(\lambda)$ represents the sample spectral reflectance, and $\bar{x}, \bar{y}, \bar{z}$ represents the colour matching function.

(b) Similarly, the tristimulus values of the halftone area are determined from the measured reflectance.

(c) Each linear combination $\vec{T}_{sum}$ of the tristimulus values $\vec{T}_{solid}, \vec{T}_{pale}, \vec{T}_{paper}$ is determined by using the weighting factors as variables, and by minimizing the squared error sum with the measured values.

$$\vec{T}_{sum} = a_s \vec{T}_{solid} + b_p \vec{T}_{pale} + (1 - a_s - b_p)\vec{T}_{paper} \qquad (7)$$

where a_s is fractional dot area of the ink, b_p is fractional dot area of the pale-ink.

(d) The chromaticity coordinates x and y are calculated from the tristimulus values.

3. Results and discussion

Figure 1 shows the spectral reflectance for the solid areas of cyan, magenta, and yellow as well as the reflectance spectrum of the paper substrate.

Figure 2 shows the change of the squared error sum between the pale-ink reflectance spectrum and the reflectance spectrum of a magenta 50% halftone area when the attenuation factor (G) due to scattering was assumed to be zero in equation (4), and the A value was varied by parameter B.

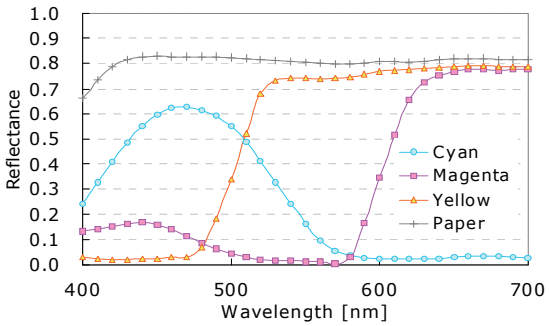

Figure 1. Spectral reflectance for the solid area of cyan, magenta, yellow and the paper substrate printed with offset printer.

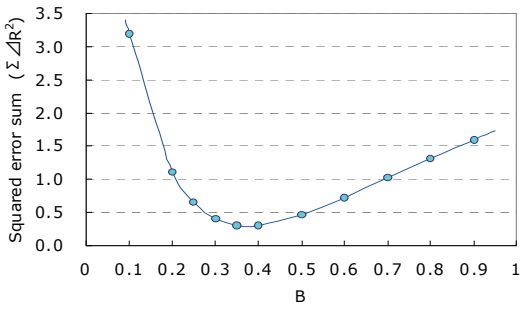

Figure 2. Squared error sum of 50% magenta halftone area spectral reflectance between the measured data and pale-ink which estimated by factor B as variable.

From this figure, it is deemed likely that the squared error sum becomes the minimum when the optical path length factor (B) is around 0.4. Based on these results, the light attenuation A that includes the attenuation factor (G) due to scattering was determined (using the method described above) for cyan, magenta, and yellow, when the optical path length factor (B) was approximately 0.4.

Table 1. The estimated values of B and G of pale-ink for cyan, magenta and yellow

	B	***G***
Cyan	0.471	0.0442
Magenta	0.376	0.0459
Yellow	0.436	0.0471
Average	0.410	0.0457

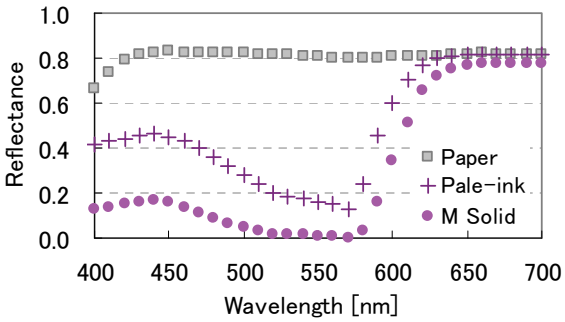

Figure 3. The estimated reflectance spectrum for the magenta pale-ink and the measured spectral reflectance for the solid area and the paper substrate.

The results are shown in Table 1.For each colour, the values B and G are close, to 0.41 for B and 0.046 for G, on average. Thus, the optical path length for the light that passes through the colorant of a halftone dot image is considered to be approximately 40% of the mean optical path length of the solid area. The cause of this is probably the lateral scattering of the incident light in both the ink and paper layers. Furthermore, judging from the G value, it is estimated that nearly 10% of the light dissipates over the entire wavelength range. Figure 3 shows the estimated reflectance spectrum for the magenta pale-ink and the measured spectral reflectance for the solid area and the paper substrate.

Figure 4 shows the estimated reflectance spectrum for the 50% halftone area of magenta pale-ink, as well as the measured spectral reflectance for the solid area, the 50% halftone area, and the paper substrate. Figure 5 shows the weighting factors, in accordance with each dot area coverage, for the solid area,

pale-ink, and the paper substrate. The estimated reflectance spectrum for the pale-ink is very close to that of the measured 50% halftone area.

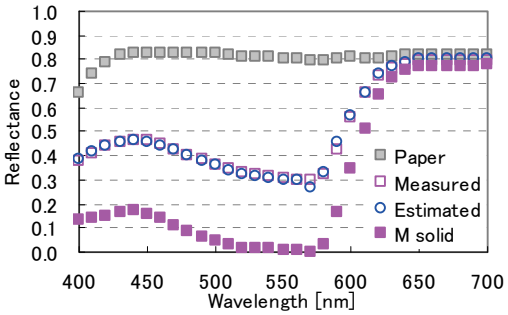

Figure 4. The estimated reflectance spectrum for the 50% halftone area of magenta pale-ink, and the measured spectral reflectance for the solid area, the 50% halftone area, and the paper.

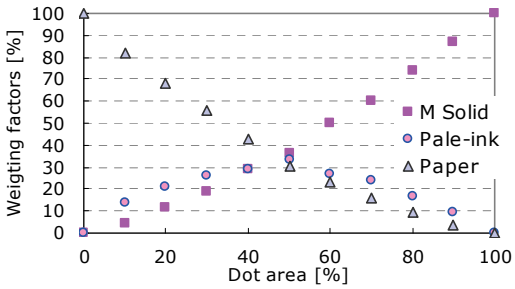

Figure 5. The weighting factors as a function of nominal dot area coverage, for the solid area, pale-ink, and the paper substrate.

The pale-ink represents the scattered light of the halftone dot area, and is considered to correspond to the optical dot gain. The weighting factor for the pale-ink in our model is parabolic, with the maximum estimated at approximately 33%. Accordingly, if the dot gain is measured at 20%, the optical dot gain is estimated at approximately 7%.

On the *xy* chromaticity coordinates shown in Fig. 6, the predicted values with the dot area coverage change of magenta ink and the illuminant D_{50} , based on the Murray-Davies, Yule-Nielsen (n=1.7), and pale-ink models are shown, along with the measured values. Table 2 shows the pale-ink chromaticity coordinates x and y for cyan, magenta, and yellow; which are calculated based on the results in Table 1. Figure 7 shows chromaticity coordinates x and y for the pale-ink model of cyan, magenta, and yellow, along with the measured values.

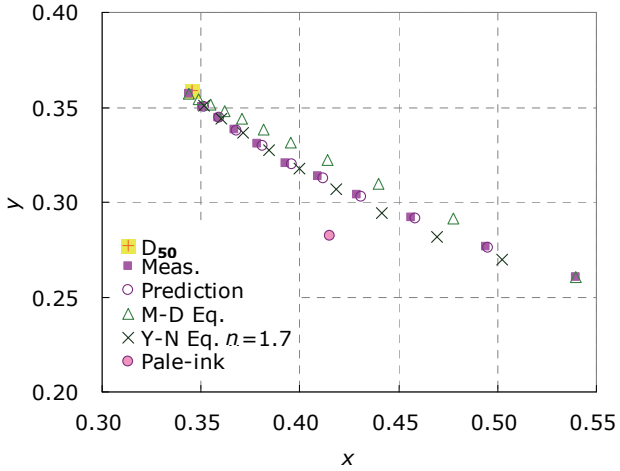

Figure 6. The predicted chromaticity coordinates with the dot area coverage change of magenta ink, based on the Murray-Davies, Yule-Nielsen, pale-ink models and the measured data.

Table 2. The calculated chromaticity coordinates of pale-ink for the cyan, magenta and yellow.

	x	*y*
Cyan	0.23	0.31
Magenta	0.41	0.28
Yellow	0.42	0.46

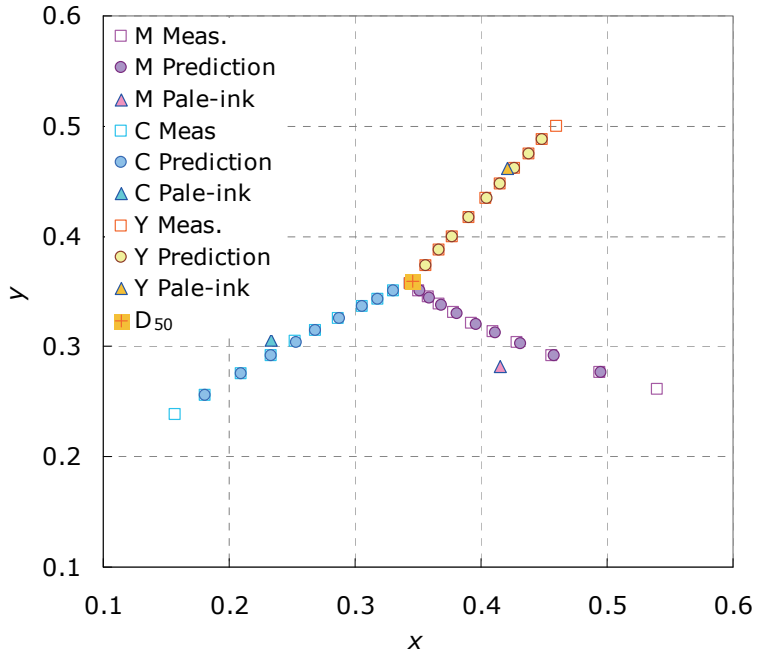

Figure 7. The chromaticity coordinates for the pale-ink model of cyan, magenta, yellow, and the measured data.

From these results, we can see that pale-ink model can accurately reproduce the change of hue in accordance with the dot area coverage. On the *xy* chromaticity diagram, the position of pale-ink is separate, in the order of magenta, cyan, and yellow, from the respective lines connecting the solid area and the paper substrate. One of the reasons for this is considered to be the presence of multiple absorption peaks in the spectra of the magenta and cyan solid areas (Fig. 1). Thus, the positions of the magenta pale-ink and cyan pale-ink seem to be separate, especially at the halftone, from the straight line. Using our pale-ink model, we found that prediction accuracy had improved over the results obtained with the conventional Murray-Davies and Yule-Nielsen models.

4. Summary

We attempted to predict dot gain, which is generated in the halftone dot pattern of reproduced photographic images, using our pale-ink model and found that our proposed model offered improved prediction accuracy over the conventional Murray-Davies and Yule-Nielsen models. The results of our examination indicate that the proposed model adequately explains the effects of the ink properties and paper substrate on optical dot gain. From a practical point of view, this model is expected to be helpful in efforts aiming at understanding the effects of dot gain on hue.

<References>

[1] Murray, A. 1936. Monochrome reproduction in photoengraving. Journal of Franklin Institute: 221-721.

[2] Yule, J.A.C. and W.J. Nielsen. 1951. The penetration of light into paper and its effect on halftone reproduction. TAGA (Technical Association of the Graphic Arts) Proceedings: 65–76.

[3] Pearson, Milton. 1980. ”n” Value for General Conditions. TAGA (Technical Association of the Graphic Arts) Proceedings: 415-425.

[4] Azuma, Y., H. Uomoto, S. Takahashi and, M. Inui. 2002. 45.Determining tone conversion characteristics of digital still camera from pictorial images without gray scale and its application to color management. Conference on Color in Graphics, Imaging and Vision (CGIV'02): 594-597.

[5] ISO TR 16066-2003, Graphic technology - Standard object colour spectra database for colour reproduction evaluation (SOCS)

[6] Delpy, D. T., M. Cope, P. van der Zee, S. Arridge, S. Wrayt, and J. Wyatt. 1988. Estimation of optical pathlength through tissue from direct time of flight measurement. Physics in Medicine and Biology 33(12): 1433-1442.

[7] CIE Publication 15.1, Colorimetry

[8] ISO 3664, Viewing condition - Graphic technology and photography.